Hydroxylation of longiborneol by a Clm2-encoded CYP450 monooxygenase to produce culmorin in Fusarium graminearum

Bahadoor, Adilah; Schneiderman, Danielle; Gemmill, Larissa; Bosnich, Whynn; Blackwell, Barbara; Melanson, Jeremy E.; McRae, Garnet; Harris, Linda J.

Publisher's version / Version de l'éditeur:
https://doi.org/10.1021/acs.jnatprod.5b00676
Journal of Natural Products, 2015-12-16

JOURNAL OF NATURAL PRODUCTS

Article

pubs.acs.org/jnp

Hydroxylation of Longiborneol by a *Clm2*-Encoded CYP450 Monooxygenase to Produce Culmorin in *Fusarium graminearum*

Adilah Bahadoor,*,† Danielle Schneiderman,† Larissa Gemmill,† Whynn Bosnich,† Barbara Blackwell,† Jeremy E. Melanson,‡ Garnet McRae,‡ and Linda J. Harris*,†

†Ottawa Research and Development Centre, Agriculture and Agri-Food Canada, Ottawa, ON K1A 0C6 Canada

‡Measurement Science and Standards, National Research Council Canada, Ottawa, ON K1A 0R6 Canada

Supporting Information

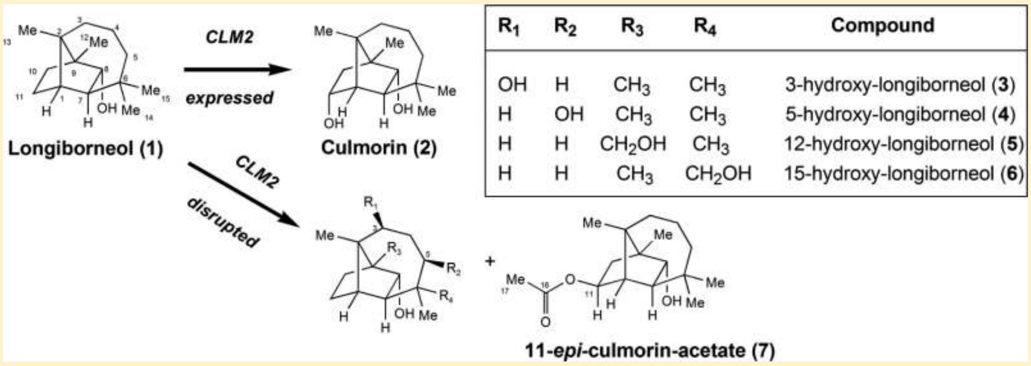

ABSTRACT: A second structural gene required for culmorin biosynthesis in the plant pathogen *Fusarium graminearum* is described. *Clm2* encodes a regio- and stereoselective cytochrome P450 monooxygenase for C-11 of longiborneol (**1**). *Clm2* gene disruptants were grown in liquid culture and assessed for culmorin production via HPLC-evaporative light scattering detection. The analysis indicated a complete loss of culmorin (**2**) from the liquid culture of the Δ*Clm2* mutants. Culmorin production resumed in a Δ*Clm2* complementation experiment. A detailed analysis of the secondary metabolites extracted from the large-scale liquid culture of disruptant Δ*Clm2*D20 revealed five new natural products: 3-hydroxylongiborneol (**3**), 5-hydroxylongiborneol (**4**), 12-hydroxylongiborneol (**5**), 15-hydroxylongiborneol (**6**), and 11-*epi*-acetylculmorin (**7**). The structures of the new compounds were elucidated by a combination of HRMS, 1D and 2D NMR, and X-ray crystallography.

■ INTRODUCTION

Culmorin is a sesquiterpene diol secondary metabolite produced largely by *Fusarium* species, namely, *F. graminearum*, *F. culmorum*, *F. venenatum* and *F. crookwellense*, in conjunction with the sesquiterpene trichothecenes of the deoxynivalenol (DON) family.[1−5] Culmorin production has also been reported in the marine ascomycete *Leptosphaeria oraemaris*.[6] In addition, the *Fusarium* species are known to produce related compounds including 5-hydroxyculmorin, 15-hydroxyculmorin, 12-hydroxyculmorin and culmorone.[4,7] While the biosynthetic pathway of the trichothecenes has been extensively studied,[8−11] culmorin and its related compounds have attracted less attention perhaps due to the lack of definitive toxicological data in past animal and cell studies.[12] However, culmorin has been identified as synergistically toxic with 4-deoxynivalenol when fed to the corn earworm, *Heliothis zea*,[13] as a phytotoxic agent in wheat coleoptile tissue,[14] and as an antifungal agent,[6,12] perhaps providing *F. graminearum* with a competitive advantage within its environmental niche. Furthermore, the persistent co-occurrence of culmorin with regulated mycotoxins, such as DON, on wheat, barley and oats[2,15] has renewed interest in the culmorin biosynthetic pathway.

Earlier studies had proposed a biosynthetic scheme, whereby farnesyl pyrophosphate was cyclized to longiborneol, the immediate precursor to culmorin.[16] *Clm1* was the first gene implicated in the biosynthesis of culmorin and encodes longiborneol synthase, a terpene cyclase responsible for the cyclization of farnesyl pyrophosphate into longiborneol.[17] This research in *F. graminearum*, as well as earlier work on *F. culmorum*, had predicted a probable enzymatic hydroxylation at C-11 of longiborneol as the last step in the culmorin biosynthesis, although this enzyme was never identified.[18]

In order to identify the hydroxylase, the candidate gene *FGSG_17598*, named *Clm2*, was disrupted and the disrupted gene then complemented by adding it back into the *F. graminearum* strain 9F1. Detailed HRMS and NMR studies on the secondary metabolites of the *Clm2* disruptant D20 (Δ*Clm2*D20), grown in liquid culture, have disclosed the identity of five new compounds **3** to **7**. Our findings suggest that *Clm2* encodes a regio- and *endo*-stereoselective cytochrome

Received: August 6, 2015

P450 (CYP450) monooxygenase for position 11 of longiborneol.

■ RESULTS AND DISCUSSION

FGSG_17598 (also known as *FGSG_00007.3*) gene expression is highly induced by agmatine as a nitrogen source and controlled by the transcriptional regulator *Tri6*, similar to other mycotoxin biosynthetic genes such as the *Tri* genes and *Clm1*.[19] Encoding a cytochrome P450, this gene was a candidate mycotoxin biosynthetic gene and was selected for characterization through gene disruption.

The 9F1 strain of *F. graminearum*, previously used in the discovery of the *Clm1*-encoded longiborneol synthase, was also chosen for this study due to its strong production of culmorin *in vitro*.[17] Disruption of *FGSG_17598* in strain 9F1 was achieved via *Agrobacterium*-mediated transformation with a *Clm2* disruption vector based on pRF-HU2 (Figure 1A).[20] Ten

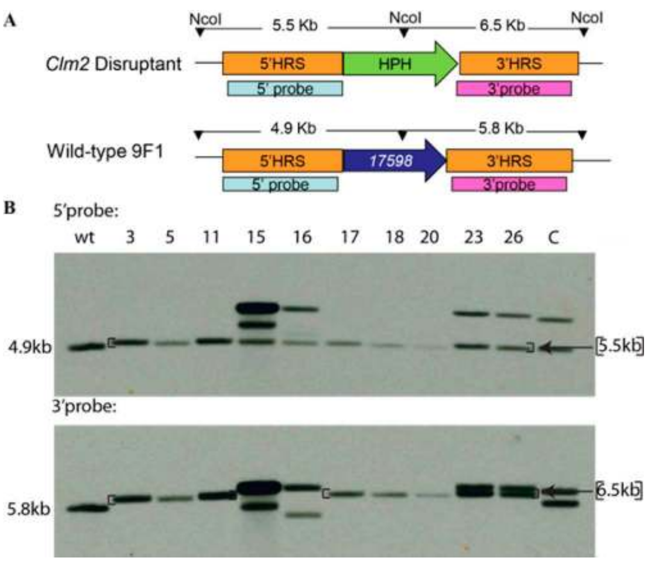

Figure 1. Structure at the *FGSG_17598* site in the genome, with expected product sizes after NcoI restriction enzyme digestions for the Δ*Clm2* disruptant and wild-type progenitor. B. Southern analysis of 10 putative *FGSG_17598* disruptants using DIG-labeled probes of 5′ and 3′ homologous recombination sequences. wt = wild-type, C = control.

independent true disruptants (Δ*Clm2*D3, 5, 11, 15, 15, 17, 18, 20, 23 and 26) and one control transformant (C) due to a single crossover event were isolated. All transformants were confirmed by PCR and Southern analysis. Figure 1B shows the Southern analysis of the 11 transformants using both the 5′ and 3′ gene flanking sequences as probes. Only the six Δ*Clm2* disruptants numbered 3, 5, 11, 17, 18, and 20 and the control C, which exhibited a simple banding pattern, were used in further analyses. We used the disruptant strain Δ*Clm2*D20 to generate 23 add-back strains in which the entire *Clm2* gene plus ~1 kb upstream and 550 bp downstream of the gene were inserted into the genome (confirmed by PCR and Southern analysis; data not shown).

The secondary metabolites produced by the wild-type progenitor and transformant strains grown in two-stage liquid culture were analyzed for culmorin at day 7 and day 12 of the second stage, by HPLC equipped with an evaporative light scattering detector (ELSD). As expected, culmorin was no longer detected from the liquid culture of Δ*Clm2*D11 and Δ*Clm2*D20 (Figure 2). Transformant control *Clm2*C, which underwent a single crossover event of the disruption vector but

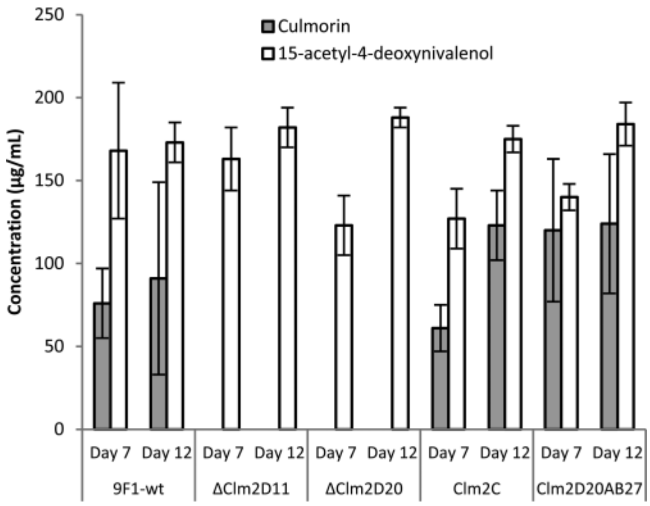

Figure 2. Culmorin and 15-acetyl-4-deoxynivalenol concentrations from 7- and 12-day-old liquid cultures of 9F1-wt, *Clm2* disruptants Δ*Clm2*D11 and Δ*Clm2*D20, transformant control *Clm2*C and add-back *Clm2*D20AB27.

retained the original *Clm2* gene sequence, maintained its ability to produce culmorin (Figure 2). Similar to the control C, the complemented strain Clm2D20AB27 produced more culmorin when compared to wild-type 9F1 (Figure 2). The disruptants, control and add-back strains produced 15-acetyl-4-deoxynivalenol on par with wild-type 9F1 (Figure 2), confirming that the trichothecene biosynthetic pathway was unaffected during the transformation process.

At this point, the culmorin profiling results of the *Clm2* disruption/add-back experiments strongly implicated the cytochrome P450 monooxygenase encoded by *Clm2* as involved in the final hydroxylation step in the biosynthesis of culmorin. To test our hypothesis, a detailed analytical study of the secondary metabolites produced by Δ*Clm2*D20 in liquid culture was conducted. Starting with an ethyl acetate extraction of a large-scale liquid growth culture of Δ*Clm2*D20, the resulting extract was fractionated via a combination of normal-phase chromatography and reversed-phase preprative-HPLC. Analysis of the eluent by LC-HRMS and NMR revealed five new natural products (**3**−**7**).

The new compounds **3** to **6** were isolated as white, crystalline solids. Compounds **3** and **4** were both identified by a major fragment $[M + H - H_2O]^+$ at m/z 221.1901 (m_{calc} 221.1900, Δm 0.45 ppm) by HRMS (Figure 3B and C). The HRMS data, along with NMR data, revealed a molecular formula of $C_{15}H_{26}O_2$ for both compounds **3** and **4**. Compounds **5** and **6** formed strong sodium adducts, $[M + Na]^+$ at m/z 261.1827 establishing their molecular formula as $C_{15}H_{26}O_2$ (m_{calc} 261.1825, Δm 0.78 ppm, Figure 3D and E). Compound **7**, a colorless oil, was identified by its $[M + NH_4]^+$ adduct at m/z 298.2384 (m_{calc} 298.2377, Δm 1.0 ppm, molecular formula $C_{17}H_{28}O_3$, Figure 3F).

Despite sharing an identical molecular formula with culmorin, each of the new compounds **3** to **6** eluted at different retention times (Figure 3A to E), thereby raising the possibility that they were isomers of culmorin. Compound **7** stood out with the presence of an acetate group, confirmed by a

DOI: 10.1021/acs.jnatprod.5b00676
J. Nat. Prod. XXXX, XXX, XXX−XXX

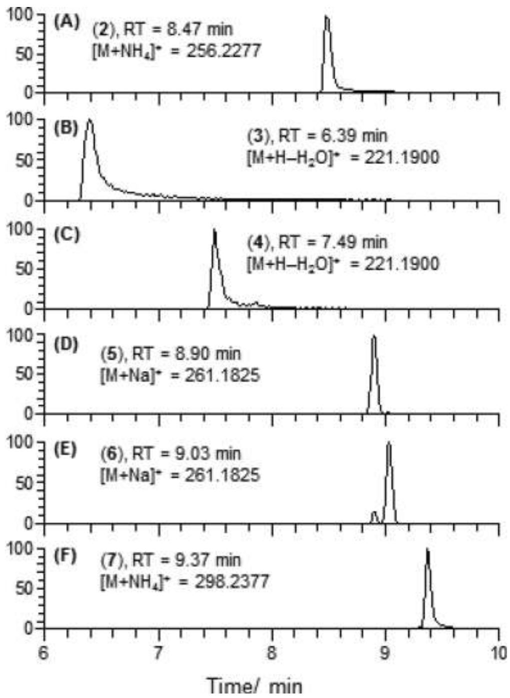

Figure 3. LC-HRMS extracted ion chromatograms of (A) culmorin (**2**), (B) 3-hydroxylongiborneol (**3**), (C) 5-hydroxylongiborneol (**4**), (D) 12-hydroxylongiborneol (**5**), (E) 15-hydroxylongiborneol (**6**) and (F) 11-*epi*-acetylculmorin (**7**). (EICs were generated with a mass window of 5 ppm centered at the calculated mass of the compound.)

neutral loss of 60 Da (CH_3COOH) by HRMS (see Supporting Information, Figure S6) and later by NMR (Table 1). It should be noted that while $[M + H]^+$ ions are commonly formed during electrospray ionization MS, these ions were generally not observed for this class of compound, consistent with other classes of compounds such as cholesterols[21] or glycerolipids[22] that lack an easily protonated site (i.e. amine group, etc.). As a result, more stable adducts with ammonium or sodium or water-loss products dominated the spectra, along with fragment ions generated in the ionization source or by breakdown of the unstable $[M + H]^+$ ions during transmission through the mass spectrometer.

Having successfully disrupted the activity of the CYP450 encoded by *Clm2*, it was perceivable that longiborneol could accumulate *in vitro*. An LC-HRMS and NMR analysis of the ethyl acetate extract of a liquid culture of mutant Δ*Clm2*D20, grown for 12 days, failed to detect any longiborneol (data not shown). It seemed that in the absence of a functional CYP450 encoded by *Clm2*, longiborneol was hydroxylated (but not at position 11) by a subset of unidentified oxygenases. The discovery of 5-hydroxyculmorin, 12-hydroxyculmorin, and 15-hydroxyculmorin in *F. culmorum*[7] and *F. graminearum*[23] all point toward unidentified oxygenases capable of oxygenating at C-5, C-12 and C-15 of the culmorin/longiborneol carboskeleton. Furthermore, the production of the hydroxyculmorin derivatives relative to culmorin varied across *Fusarium* species.[3] *F. culmorum* isolates produced more 5-hydroxyculmorin and 15-hydroxyculmorin than culmorin, whereas *F. graminearum* isolates produced more culmorin than 5-hydroxyculmorin and 12-hydroxyculmorin.[3]

In wild-type *F. graminearum* 9F1, the presence of 5-, 12-, and 15-hydroxyculmorin, detectable in the extracted ion chromatogram (EIC) (Figure 4B), was dwarfed by the high abundance of culmorin (**2**) (Figure 4A), suggesting that in this strain the *Clm2*-encoded CYP450 displayed superior enzymatic activity to the unidentified, possibly promiscuous C-5, C-12, and C-15 oxygenases. Assuming *Clm2* encodes an exclusive CYP450 oxygenase, its disruption would leave the possibly nonspecific C-5, C-12, and C-15 oxygenases fully functional and still able to hydroxylate longiborneol. It is therefore conceivable that the new compounds **3** to **7** were the products of these hydroxylases. If this were the case, compounds **3** to **7** could

Table 1. NMR Spectroscopic Data ($CDCl_3$) for 3-Hydroxylongiborneol (3) and 5-Hydroxylongiborneol (4)

	3[a]		4[b]	
position	δ_C, type	δ_H (J in Hz)	δ_C, type	δ_H (J in Hz)
1	42.6, CH	1.91 d (4.3)	43.8, CH	1.87 d (4.5)
2	55.6, C		49.7, C	
3	73.4, CH	3.56 dd (2.3, 7.6)	30.8, CH_2	β: 1.31–1.34 (m)
				α: 1.38–1.42 (m)
4	33.3, CH_2	β: 1.72–1.79 (m)	31.6, CH_2	β: 1.66–1.74 (m)
		α: 1.63–1.67 (m)		α: 1.52 dd (13.7, 6.7)
5	35.7, CH_2	β: 1.51–1.56 (m)	79.5, CH	3.34 dd (11.6, 1.7)
		α: 1.17–1.30 (m)		
6	29.7, C		37.3, C	
7	64.6, CH	1.00 d (4.8)	64.6, CH	1.06 (s)
8	79.5, CH	3.83 dd (4.8, 2.0)	78.2, CH	3.68 d (4.7)
9	51.4, C		51.3, C	
10	26.2, CH_2	*exo*: 1.17–1.30 (m)	26.2, CH_2	*exo*: 1.20–1.13 (m)
		endo: 1.90–1.96 (m)		*endo*: 1.85–1.82 (m)
11	30.4, CH_2	*exo*: 1.72–1.79 (m)	30.3, CH_2	*exo*: 1.74–1.66 (m)
		endo: 1.17–1.30 (m)		*endo*: 1.13–1.20 (m)
12	13.2, CH_3	0.90 (s)	12.9, CH_3	0.83 (s)
13	15.3, CH_3	0.94 (s)	22.4, CH_3	0.84(s)
14	30.1, CH_3	0.92 (s)	21.1, CH_3	0.89 (s)
15	27.2, CH_3	0.93 (s)	26.7, CH_3	1.06 (s)

[a] ^{1}H NMR recorded at 500 MHz and ^{13}C NMR recorded at 125 MHz. [b] ^{1}H NMR recorded at 600 MHz and ^{13}C NMR recorded at 150 MHz.

DOI: 10.1021/acs.jnatprod.5b00676
J. Nat. Prod. XXXX, XXX, XXX–XXX

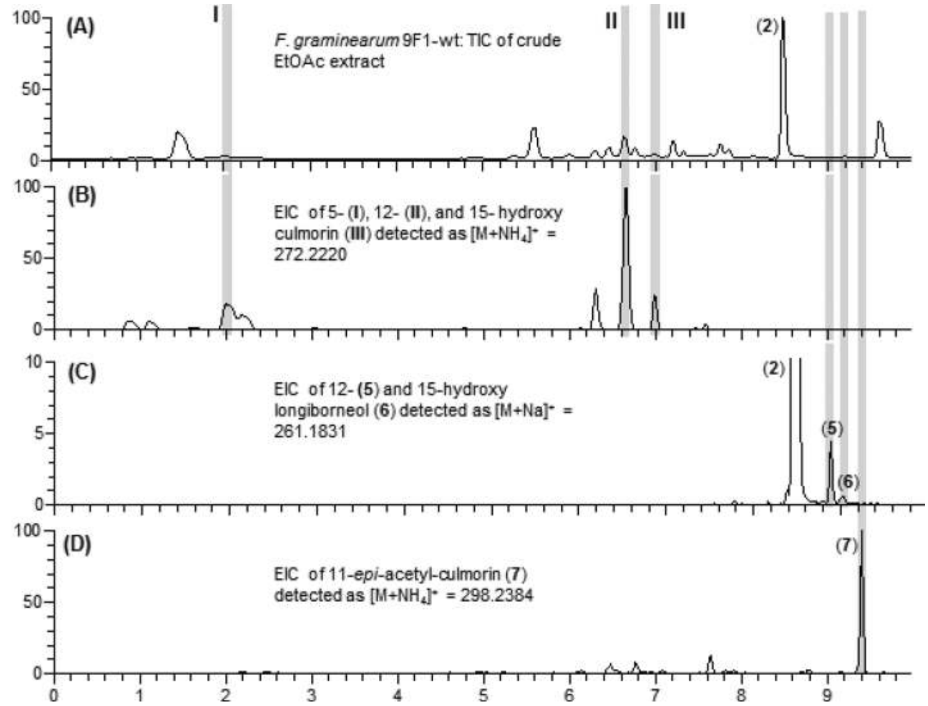

Figure 4. LC-HRMS analysis of the crude EtOAc extract of a 12-day liquid culture of wild-type *F. graminearum* 9F1: (A) TIC of the crude EtOAc extract showing an abundance of culmorin (**2**, t_R = 8.47 min, m/z = 256.2273 $[M + NH_4]^+$) compared to (B) 5-, 12-, and 15-hydroxyculmorin represented by compounds **I** (t_R = 2.00 min), **II** (t_R = 6.65 min), and **III** (t_R = 6.99 min), (C) EIC of 12- and 15-hydroxylongiborneol with 10× magnification of the y-axis (**5**, t_R = 8.89 min; **6**, t_R = 9.03 min), and (D) the EIC of 11-*epi*-acetylculmorin (**7**, t_R = 9.40 min). (EICs were generated with a mass window of 5 ppm centered at the calculated mass of the compound.)

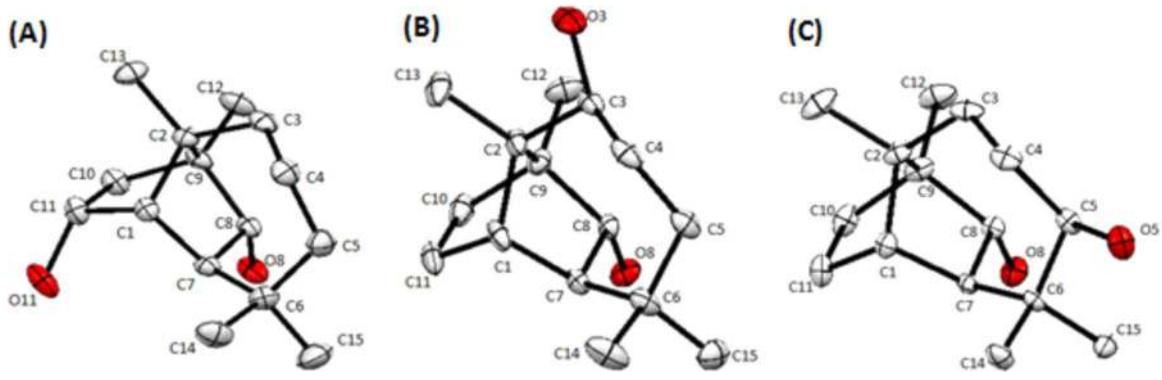

Figure 5. ORTEP representations of (A) culmorin (**2**), (B) 3-hydroxylongiborneol (**3**), and (C) 5-hydroxylongiborneol (**4**). Hydrogen atoms are omitted for clarity, and thermal ellipsoids are scaled to 30% of the overall electron density.

be among the minor metabolites of wild-type 9F1, which had so far evaded detection. Indeed, an LC-HRMS analysis identified the sodium adducts of compounds **5** and **6** in the EtOAc extract of the 12-day liquid culture of wild-type 9F1 (Figure 4C). Compound **7** produced an easily detectable ammonium adduct (Figure 4D). Unfortunately, compounds **3** and **4**, which most likely ionize poorly, were not detected.

A full array of NMR experiments, including, ^{1}H, ^{13}C, COSY, HSQC, HMBC, 1D-NOE, and NOESY (Table 1 and Supporting Information) was performed, which determined that compounds **3** to **7** possessed an *endo*-hydroxy group at position 8, as seen in longiborneol. This observation is consistent with the proposed culmorin biosynthetic pathway, which envisaged an *endo*-hydroxylation at position 8 as the termination step of the cyclization of farnesyl pyrophosphate to the longiborneol carbo-skeleton.[17,24] However, the position of the second hydroxylation site varied and was determined as described below.

The ^{1}H NMR (Table 1) and phase-sensitive HSQC spectrum of compounds **3** and **4** revealed several similar features: each had two downfield methine protons (H3 and H8 for **3**; H5 and H8 for **4**) consistent with the presence of two hydroxy groups and four methyl groups as indicated by four prominent singlets (positions 12, 13, 14, and 15) each integrating for three protons. A combination of COSY, HMBC and NOE experiments eventually confirmed the presence of a second hydroxy group at C-3 in compound **3** and at C-5 in compound **4**. In the COSY spectrum of **3**, a definitive coupling between H-3 and H-4$_\beta$ was discerned. Key three-bond coupling between H-3 and C1, C9, C5 and C13 in the HMBC of **3** confirmed the position of the hydroxy group at position 3 (Table S1). The stereochemistry of H-3 in an α

Table 2. NMR Spectroscopic Data ($CDCl_3$) for 12-Hydroxylongiborneol (5), 15-Hydroxylongiborneol (6) and 11-*epi*-Acetylculmorin (7)

	5[a]		6[a]		7[b]	
position	δ_C, type	δ_H (J in Hz)	δ_C, type	δ_H (J in Hz)	δ_C, type	δ_H (J in Hz)
1	44.8, CH	1.84 d (4.4)	43.9, CH	1.83 d (4.4)	49.5, CH	2.08 (s)
2	50.5, C		50.6, C		50.0, C	
3	35.7, CH_2	β: 1.34−1.37 (m) α: 1.41−1.44 (m)	34.9, CH_2	α and β: 1.33−1.42 (m)	36.1, CH_2	α and β: 1.23−1.46 (m)
4	22.5, CH_2	α and β: 1.41−1.44 (m)	22.2, CH_2	α and β: 1.43−1.52 (m)	21.4, CH_2	α and β: 1.23−1.46 (m)
5	41.0, CH_2	α and β: 1.34−1.37 (m)	35.4, CH_2	β: 1.43−1.52 (m) α: 1.18−1.23 (m)	41.1, CH_2	α and β: 1.23−1.46 (m)
6	33.3, C		37.8, C		33.3, C	
7	64.1, CH	1.01 d (4.6)	59.7, CH	1.18−1.23 (m)	61.5, CH	0.87 d (4.8)
8	79.2, CH	4.22 dd (4.6, 1.8)	79.4, CH	3.90 dd (5.0, 1.7)	78.0, CH	3.73 dd (4.8, 1.8)
9	54.6, C		50.9, C		52.1, C	
10	23.3, CH_2	*exo*: 1.34−1.37 (m) *endo*: 2.25 ddd (12.8, 9.1, 4.7)	26.3, CH_2	*exo*: 1.18−1.23 (m) *endo*: 1.85 ddd (14.0, 9.0, 3.1)	36.1, CH_2	*exo*: 1.23−1.46 (m) *endo*: 2.40 dd, (14.3, 8.3)
11	30.0, CH_2	*exo*: 1.75−1.80 (m) *endo*: 1.24−1.32 (m)	30.6, CH_2	*exo*: 1.73 ddd (17.6, 6.8, 4.4) *endo*: 1.18−1.23 (m)	78.7, CH	*endo*: 4.56 dd (8.3, 3.3 Hz)
12	66.4, CH_2	a: 3.89 d (10.3) b: 3.68 d (10.3)	13.0, CH_3	0.84 (s)	12.3, CH_3	0.89 (s)
13	22.9, CH_3	0.84 (s)	22.5, CH_3	0.83 (s)	21.3, CH_3	0.98 (s)
14	29.03, CH_3	0.92 (s)	24.0, CH_3	0.87 (s)	28.8, CH_3	0.96 (s)
15	28.99, CH_3	0.93 (s)	72.3, CH_2	a: 3.46 d (11.3) b: 3.28 d (11.3)	29.5, CH_3	0.94 (s)
16					170.6, C	
17					22.2, CH_3	1.99 (s)

[a] ^{1}H NMR recorded at 600 MHz and ^{13}C NMR recorded at 150 MHz. [b] ^{1}H NMR recorded at 500 MHz and ^{13}C NMR recorded at 125 MHz.

orientation was established by a 1D-NOE experiment, which identified clear NOE interactions between H-3 and H-8 and CH_3-12 (Figure S13). Likewise, in compound **4**, a strong coupling between H-5 and H-4_β in the COSY spectrum and three-bond coupling between H-5 and C-14 and C-15 observed by HMBC indicated the presence of the hydroxy group at position 5 (Table S1). Observed NOE interactions between H-5 and H-8 and CH_3-15 established an α orientation for H-5 (Figure S13). X-ray crystallography data obtained on compounds **3** (CCDC deposition number 1412299, Figure 5B) and **4** (CDCC deposition number 1412298, Figure 5C) corroborated the interpretation of the 1D and 2D NMR experiments to establish their fully elucidated structures. The X-ray crystal structure of culmorin (CDCC deposition number 1412297), which to our knowledge has not yet been reported, is also displayed to offer an unbiased comparison (Figure 5A). Taken together, the 2D NMR and X-ray crystallography data provided enough evidence to name compounds **3** and **4** 3-hydroxylongiborneol and 5-hydroxylongiborneol, respectively.

A similar process to that described above was followed to decipher the full structure of compounds **5** and **6**. A combination of ^{1}H NMR (Table 2) and phase sensitive HSQC experiments revealed that one of the methyl groups in both **5** and **6** was hydroxylated. The AB methylene protons from the CH_2OH unit resulting from the hydroxylation of the methyl function was easily distinguished from a COSY spectrum and displayed distinct HMBC correlations that enabled the location of the hydroxylated methyl group in both **5** and **6** (Table S1). In compound **5**, three-bond heteronuclear coupling between the AB system of H-12a/H-12b and C-10 and C-8 illustrated that hydroxylation had occurred on C-12 (Table S1). Finally, observed NOE interactions between H-12a and H-3_α in compound **5** (Figure S13) confirmed its structure as 12-hydroxylongiborneol.

In compound **6**, hydroxylation had occurred on C-15 based upon three-bond heteronuclear coupling observed between the AB system H-15a/H-15b and C-5, C-7 and C-14 (Table S1) and NOE interactions. Two distinct NOE interactions were used to discriminate between positions 14 and 15 as the hydroxylation site. First, a unique NOE interaction between CH_3-14 and H-1 (Figure S13) confirmed that no hydroxylation had occurred at position14, leaving position 15 as the only site for hydroxylation to occur. Second, both protons of the AB system (H-15a/H-15b) produced clear NOE interactions with CH_3-14 (Figure S13) to establish compound **6** as 15-hydroxylongiborneol.

Up to this point, the fully elucidated structures of hydroxylongiborneol derivatives **3** to **6** had provided sufficient evidence to designate the *Clm2*-encoded CYP450 as a regioselective monooxygenase for position 11. However, it was the structure elucidation of compound **7** that revealed its *endo*-stereoselectivity. Focusing on H-11, which by its characteristic δ_H of 4.56 ppm and distinct three-bond coupling in the HMBC between H-11 and C-7, C-9, and C-16, indicated its attachment to C-11 and also confirmed the location of the acetate group (Table 2, Table S1). Unlike culmorin (**2**) where H-11 is *exo*, in compound **7** three strong NOE interactions observed between H-11 and H-1, H-7 and *endo*-H-10 were possible only if H-11 conformed to an *endo* spatial orientation (Figure 6). As a result, it was unequivocally deduced that to produce culmorin (**2**) with its characteristic C-11 *endo*-hydroxy group, the CYP450 encoded by *Clm2* must be both a regio- and *endo*-stereoselective oxygenase for C-11 of longiborneol.

Since we were not able to produce a crystal structure of compound **7** for additional proof of structure, culmorin was

DOI: 10.1021/acs.jnatprod.5b00676
J. Nat. Prod. XXXX, XXX, XXX−XXX

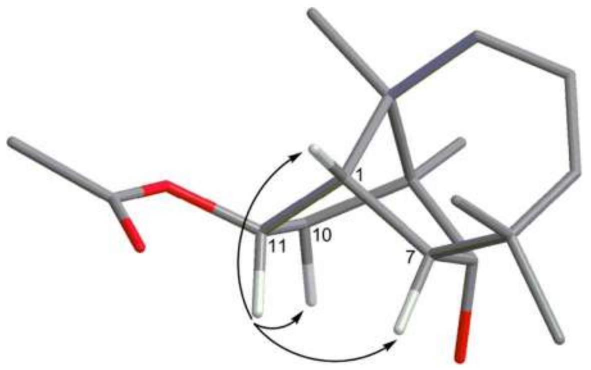

Figure 6. Relevant 1D-NOE correlations of *endo* H-11 in 11-*epi*-acetylculmorin (**7**).

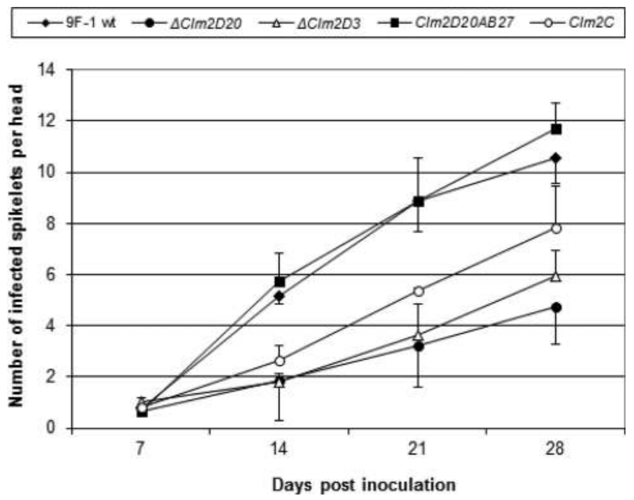

Figure 7. Virulence assay on Roblin wheat heads after inoculation with Δ*Clm2*D3, Δ*Clm2*D20, *Clm2*D20AB27, *Clm2*C and wild-type 9F-1 macroconidia.

acetylated to produce a mixture of 11-acetylculmorin (**8**) and 8-acetylculmorin (**9**) (see Supporting Information, p S19). The LC-HRMS (Figures S6, S7, S8) and ^{1}H and ^{13}C spectra (pp S13−S15 and Table S6) of synthesized 11-acetylculmorin (**8**) and 8-acetylculmorin (**9**) showed distinct differences from 11-*epi*-acetylculmorin (**7**). The discovery of 11-*epi*-acetylculmorin (**7**) also pointed to the existence of an oxygenase capable of installing a C-11 *exo*-hydroxy group in longiborneol, whose activity was not apparent until *Clm2* was disrupted in wild-type 9F1. It appeared that this oxygenase maintained its activity in wild-type 9F1, which produced **7** *in vitro* (Figure 4D). To confirm our hypothesis, a search for an 11-deacetyl version of **7** from both the liquid culture extract of wild-type 9F1 and disruptant Δ*Clm2*D20 is currently under way.

The discoveries of 3-, 5-, 12- and 15-hydroxylongiborneol and 11-*epi*-acetylculmorin, along with the discovery of 14-hydroxylongiborneol, named isoculmorin, from the marine fungi *Kallichroma tethys*,[25] indicated that hydroxylation on the longiborneol/culmorin carbo-skeleton was ubiquitous, with a number of hydroxylases involved in the process. Our findings suggest that one member of this hydroxylase family, a CYP450 encoded by *Clm2*, is a regio- and *endo*-stereoselective enzyme for C-11.

With a number of *Clm2* disruptants available, which no longer produced culmorin, we investigated the virulence of the disruptants *in planta*. The impact on virulence of 4-deoxynivalenol, the major trichothecene derived from the acetyldeoxynivalenol produced by *F. graminearum*, is well-documented.[26−28] Even though culmorin is frequently detected on wheat heads highly contaminated with 4-deoxynivalenol,[2,3,15] its role as a disease-causing agent has not been investigated. Here, two disruptants, Δ*Clm2*D3 and Δ*Clm2*D20, the transformant control *Clm2*C and the add-back *Clm2*D20AB27 were chosen for a wheat virulence assay. Disease progression was followed over 7, 14, 21 and 28 days (Figure 7) and results were analyzed by ANOVA. At day 14 through day 28, both Δ*Clm2*D3 and Δ*Clm2*D20 had significantly reduced virulence in comparison to the wild-type 9F1 and add-back *Clm2*D20AB27, which produced very similar infection levels ($p < 0.05$). However, Δ*Clm2*D3 was not significantly different from the control transformant (*Clm2*C), which exhibited virulence intermediate between the wild-type and the disruptants. The results are in contrast with Gardiner et al. who reported disrupting *FGSG_00007* (revised gene model now known as *FGSG_17598*) in the Australian *F. graminearum* strain CS3005 and reported increased virulence of these gene disruptants relative to the wild-type progenitor in wheat heads.[19] This may be due to the different genetic backgrounds of the two original wild-type strains used for transformation and wheat hosts.

This report extends the research initiated by McCormick et al.[17] to elucidate the biosynthetic pathway to culmorin. The previously reported terpene cyclase encoded by *Clm1* cyclizes farnesyl pyrophosphate to longiborneol,[17] which in turn is hydroxylated in a regio- and *endo*-stereoselective manner at position 11 by a CYP450 encoded by *Clm2* to produce culmorin. The characterization of *Clm1* and *Clm2* has provided the means to better assess the role of culmorin in virulence or other aspects of fungal biology.

■ EXPERIMENTAL SECTION

General Experimental Procedures. 1D and 2D NMR spectra were recorded on either a Bruker Avance NMR spectrometer at 500 MHz or a Bruker Avance III NMR spectrometer at 600 MHz, equipped with a cryoprobe. Chemical shifts were referenced to residual $CDCl_3$ peaks at δ_H 7.24 ppm for ^{1}H and δ_C 77.0 ppm for ^{13}C. LC-HRMS analyses were performed on an Agilent 1260 HPLC coupled to a ThermoFisher LTQ-Orbitrap Hybrid mass spectrometer. Elution (0.3 mL/min) was carried out on a reversed-phase Kinetex column (C_{18}, 50 × 2.1 mm, 1.7 μm) heated to 40 °C, using a methanol−water mobile phase containing 5 mM ammonium acetate with the following gradient: 0.10−0.50 min (30% MeOH), 0.50−7.50 min (30−90% MeOH), 7.50−10.50 min (90% MeOH), 10.50−10.60 min (90−30% MeOH), and 10.60−16.00 min (30% MeOH). High resolution mass spectral data were recorded in positive mode for a scan range of m/z = 100−1000, at a resolution of 60 000 and a maximum linear trap fill-time of 100 ms, except for compounds **3** and **4**, where the scan range was narrowed to m/z = 150−300 and the maximum linear trap fill-time increased to 1000 ms. The ESI source operated at a capillary voltage of 10 V, tube lens voltage of 55 V, capillary temperature of 350 °C, spray voltage of 4 kV, sheath gas flow of 45 units, auxiliary gas flow of 25 units, and heater temperature of 350 °C. HPLC-ELSD analyses were accomplished on a Shimadzu system equipped with an LC-20AB pump and an ELSD-LT II detector operating at 40 °C, a nitrogen pressure of 45 psi, and gain set at 7. The samples eluted at 1 mL/min on a Kinetex column (C_{18}, 150 × 4.6 mm, 5 μm) using the following CH_3CN−water gradient: 0.01−14.00 min (5−60% CH_3CN), 14.00−15.00 min (60−100% CH_3CN), 15.00−17.00 min (100% CH_3CN), 17.00−18.00 min (100−5% CH_3CN), and 18.00−25.00 min (5% CH_3CN). Preparative HPLC separation was carried out on a 1260 Agilent system equipped with a Kinetex Axia column (C_{18}, 100 × 21.2

DOI: 10.1021/acs.jnatprod.5b00676
J. Nat. Prod. XXXX, XXX, XXX−XXX

mm, 5 μm), eluting at 20 mL/min and using a CH_3CN−water gradient (0−14 min (10−60% CH_3CN), 14−16 min (60−100% CH_3CN), 16−19 min (100% CH_3CN), 19−21 min (100−10% CH_3CN), 21−24 min (10% CH_3CN)) for compounds **3**, **4**, and **7** and a MeOH−water gradient (0−1 min (40% MeOH), 1−4 min (40−78% MeOH), 4−6.5 min (78−85% MeOH), 6.5−7 min (85−100% MeOH), 7−9.5 min (100% MeOH), 9.5−10 min (100−40% MeOH), 10−16 min (40% MeOH)) for compounds **5** and **6**. Fractions were screened by LTQ Orbitrap and ^{1}H NMR. Optical rotation data were obtained from an Atago AP-300 polarimeter, and the melting point was recorded on an Electrothermal melting point apparatus.

Generation of Transformation Vectors. A *FGSG_17598* disruption vector was constructed with the USER pRF-HU2 vector system containing the hygromycin resistance gene (*hygR*) for selection.[29] Primers were designed to amplify 998 bp of the promoter (5′ region; primer 5&6 in Table S5) and 547 bp of the 3′ region (primer 7&8 in Table S5) downstream of the gene, including sequence overhangs (underlined sequence, Table S5) to facilitate cloning into the vector.

An *FGSG_17598* add-back transformation vector was constructed with the pRF-GU vector containing the neomycin phosphotransferase II gene (nptII), conferring resistance to Geneticin (G418 sulfate).[29] Primers (9&10, Table S5), with added overhangs (underlined sequence), were used to amplify a 3.0 kb fragment encompassing the entire *FGSG_17598* gene including 998 bp upstream and 547 bp downstream of the coding region.

PCR amplification for both the disruption and add-back vector constructs was performed using Pfu Turbo Cx Hotstart DNA polymerase (Stratagene). For both the disruption and add-back system, the pRF-HU2 and pRF-GU vectors were linearized by restriction digest using Pac I followed by digestion with Nt.BbvCI (New England Biolabs). For the disruption system, the amplified upstream regions (250 ng) and downstream regions (250 ng) were cloned into the linearized pRF-HU2 vector fragments (100 ng) using the USER enzyme mix (New England Biolabs). For the add-back system, the amplified PCR product (3.0 Kb) (250 ng) was ligated to the linearized pGU vector (100 ng) using the same USER enzyme mix. In both systems, after a 37 °C incubation for 20 min, followed by 25 °C for another 20 min, the reaction mix was diluted 5× with Tris-EDTA buffer pH 8.0 and transformed into chemically competent Top 10 cells (Invitrogen). PCR screening of the resultant clones was carried out using primers to amplify both the upstream (5&6) and downstream (7&8) regions (disruption vector construct) and gene-specific primers (1&2, Table S5) in the add-back system.

***A. tumefaciens*-Mediated Transformation and Analysis of Transformants.** The disruption and add-back vectors were transformed into electro-competent *Agrobacterium* cells as previously described.[20] *F. graminearum* spores were prepared by growing mycelia on half-strength potato dextrose (1/2 PDA) agar plates for 3−5 days at 25 °C under fluorescent and black light to induce sporulation. Spores were collected as described previously.[30] *FGSG_17598* was disrupted in *F. graminearum* strain 9F1 (DAOM 240757, Canadian Collection of Fungal Cultures, Ottawa, ON, Canada) and restored in the *F. graminearum* Δ*Clm2*D20 (DAOM 241173) strain using an *Agrobacterium*-mediated system.[20] Selection of putative gene disruptants was conducted using 150 μg/mL of hygromycin B, and gene add-back selection was done using 150 μg/mL of Geneticin.

Screening of putative disruptants was done using PCR analysis on genomic DNA extracted from mycelial tissue (grown on potato dextrose agar and extracted using the EZNA Fungal DNA Isolation Kit, Omega Biotek [Norcross]). Gene-specific primers were used for PCR screening and single spores were isolated from all PCR-positive disruptants, as previously described.[31] Southern analysis was performed using 10 μg of genomic DNA extracted with the Illustra DNA Extraction Kit (GE Health Care) and digested with the restriction enzyme *NcoI* (New England Biolabs). The hybridization probes (amplified regions upstream and downstream of the disrupted gene) were generated using the PCR DIG labeling kit and hybridizations done using the DIG Detection Kit (Roche Applied Science), as per manufacturer's instructions.

Liquid Culture of 9F1-wt, *Clm2* Transformants, and HPLC Analyses. Strains of 9F1-wt, Δ*Clm2*D11, Δ*Clm2*D20, *Clm2*C, and *Clm2*D20AB27 were grown in three separate biological replicate experiments, using a two-stage liquid fermentation system modified from Miller and Blackwell.[32] Six flasks of each strain were grown during each replicate growth (for a total of 30 flasks for each experiment). Each flask also contained a circular piece (70 mm in diameter) of Miracloth (Calbiochem), which provided support for the fungal biomass. First-stage medium designed to bulk up mycelia (50 mL in 250 mL flasks) was inoculated with 1 mL of 1 × 10^8 spores/mL into each flask and grown in the dark with shaking (180 rpm, 2.5 cm throw) at 28 °C. After 48 h the first-stage medium was pipetted out of the flask, leaving the fungal mycelia on the Miracloth. The fungal mycelia/Miracloth was rinsed with approximately 10 mL of second-stage medium[32] in the original flask, the wash was pipetted off and 50 mL of fresh second stage medium was added to each flask. Flasks were then placed back on the shaker under the same conditions and left to grow for 12 days. Samples of 1 mL were taken on days 7, 10, and 12. Day 12 samples were taken after the medium from each strain was pooled.

After 12 days of growth, flasks of each strain were pooled by removing fungal growth and combining the media. The media was suspended on Chem Elut columns (Agilent) and extracted with three volumes of ethyl acetate. The ethyl acetate extract was then dried down, the extract was weighed and a ^{1}H NMR of each was taken to confirm HPLC-ELSD results.

For a large scale culture of Δ*Clm2*D20, 24 × 250 mL flasks were fitted with glass filters (70 mm in diameter, GE Healthcare), and the same two stage culture protocol as described above was performed. The Miracloth was replaced by glass filters since it was observed that the coating of the Miracloth interfered with the ethyl acetate extraction. After 12 days in second-stage medium,[32] the media from the 24 flasks were combined to a total of 1.2 L and extracted as described below. The material to examine the 9F1-wt was obtained in the same way.

Extraction and Isolation. Liquid−liquid extraction of the crude fungal filtrate (1.2 L) was performed with ethyl acetate. The organic layer was washed with brine, dried over anhydrous sodium sulfate, filtered and reduced under vacuum. The crude oily residue (1.5 g) was divided into three 500 mg portions and each portion separated by normal phase chromatography on prepacked silica gel cartridges (Supelco, 12 g, 60A), eluting successively with 100% hexanes (100 mL), 5% EtOAc−hexanes (100 mL), 10% EtOAc−hexanes (50 mL), 15% EtOAc−hexanes (50 mL), 20% EtOAc−hexanes (50 mL), 25% EtOAc−hexanes (50 mL), 30% EtOAc−hexanes (50 mL), 35% EtOAc−hexanes (50 mL), 40% EtOAc−hexanes (50 mL), 50% EtOAc−hexanes (50 mL), 60% EtOAc−hexanes (50 mL), 70% EtOAc−hexanes (50 mL), 80% EtOAc−hexanes (50 mL), and 100% EtOAc−hexanes (100 mL). Each of the individual fractions above was reduced under vacuum. Preparative HPLC separation of the 15% EtOAc−hexanes fraction afforded compound **7** (3 mg), the 20% EtOAc−hexanes and 25% EtOAc−hexanes fractions produced compounds **3** (10 mg), **5** (4 mg) and **6** (0.9 mg) and the 30% EtOAc−hexanes fraction produced compound **4** (9 mg).

*3-Hydroxylongiborneol (**3**).* Lyophilized preparative HPLC fractions were combined and recrystallized in CH_2Cl_2, producing crystals with a melting point of 164.5 °C and $[\alpha]^{25}_D$ −22.7 (*c* 0.44, CH_3Cl). Crystallographic data have been deposited in the Cambridge Crystallographic Data Centre (deposition number CCDC 1412299, available at www.ccdc.cam.ac.uk/products/csd/request).

*5-hydroxylongiborneol (**4**).* Lyophilized preparative HPLC fractions were combined and recrystallized in CH_2Cl_2, producing crystals with a melting point of 194 °C and $[\alpha]^{25}_D$ +33.3 (*c* 0.6, CH_3Cl). Crystallographic data have been deposited in the Cambridge Crystallographic Data Centre (deposition number CCDC 1412298, available at www.ccdc.cam.ac.uk/products/csd/request).

*12-Hydroxylongiborneol (**5**) and 15-Hydroxylongiborneol (**6**).* Compounds **5** and **6** coeluted during the preparative HPLC separation using the CH_3CN−water gradient. Fractions containing compounds **5** and **6** were combined and repurified using the MeOH−water gradient (see General Experimental Procedures). 12-Hydroxylongiborneol (**5**) coeluted with about 5% of compound **6** according to ^{1}H NMR and dried to a white solid with a melting point of 108−111 °C and $[\alpha]^{25}_D$ −23.8 (*c* 0.4, MeOH). 15-Hydroxylongiborneol (**6**) coeluted with about 25% of compound **5** according to ^{1}H NMR and was recrystallized in petroleum ether−EtOAc for further purification. The resulting crystals had a melting point of 111 °C and $[\alpha]^{25}_D$ −23.8 (*c* 0.09, MeOH).

11-epi-Acetylculmorin (7). Lyophilized preparative HPLC fractions produced a colorless oil with an $[\alpha]^{25}_D$ +47.6 (*c* 0.2, CH_3Cl).

Virulence Assay. Spring wheat (*Triticum aestivum* cultivar AC Roblin) was grown in growth cabinets under a 22 °C/16 °C 16 h day/8 h night cycle. One spikelet per wheat head was inoculated at midanthesis with 1000 macroconidia from *F. graminearum* wild-type 9F1, Δ*Clm2*D3, Δ*Clm2*D20, Δ*Clm2*D20AB27 and *Clm2*C. After inoculation, plants were kept in a misting chamber with 15 s misting every 30 min for the first 2 days, followed by misting every 4 h during the day cycle. Three biological replicates were completed with 10−15 wheat heads inoculated per strain for each replicate and disease scoring was conducted at 7, 14, 21 and 28 days postinoculation. Analysis of variance was performed using the REML option of the PROC MIXED procedure of SAS 9.3 (SAS Institute, Cary, NC, USA).

■ ASSOCIATED CONTENT

Supporting Information

The Supporting Information is available free of charge on the ACS Publications website at DOI: 10.1021/acs.jnatprod.5b00676.

> HRMS and NMR spectra for all compounds mentioned, HMBC data (Table S1), NOE data, X-ray crystallographic data for culmorin (**2**) (Table S2) and compounds **3** (Table S3) and **4** (Table S4), description of primers (Table S5), NMR data for compounds **8** and **9** (Table S6), ANOVA analysis (Table S7), and supplementary experimental procedures (PDF)

■ AUTHOR INFORMATION

Corresponding Authors

*Phone (A. Bahadoor): 613 759 7640. E-mail: adilah.bahadoor@agr.gc.ca.

*Phone (L. J. Harris): 613 759 1314. E-mail: linda.harris@agr.gc.ca.

Notes

The authors declare no competing financial interest.

■ ACKNOWLEDGMENTS

This project was supported by funding from the Agriculture & Agri-Food Canada Growing Forward 2 program, grant number J-000048. We are grateful to Dr. Yves Aubin from Health Canada (Ottawa, Canada) for NMR assistance on the Bruker Avance III 600 MHz NMR, Dr. Ilia Korobkov from the University of Ottawa (Ottawa, Canada) for solving the X-ray crystallography structure and Dr. Aida Kebede for statistical analysis.

■ REFERENCES

(1) Foster, B. C.; Neish, G. A.; Lauren, D. R.; Trenholm, H. L.; Prelusky, D. B.; Hamilton, R. M. G. *Microbiol., Aliments, Nutrition* **1986b**, *4*, 199−203.

(2) Ghebremeskel, M.; Langseth, W. *Mycopathologia* **2001**, *152*, 103−108.

(3) Langseth, W.; Ghebremeskel, M.; Kosiak, B.; Kolsaker, P.; Miller, D. *Mycopathologia* **2000**, *152*, 23−34.

(4) Miller, J. D.; McKenzie, S. *Mycologia* **2000**, *92*, 764−771.

(5) Lauren, D. R.; Ashley, A.; Blackwell, B. A.; Greenhalgh, R.; Miller, J. D. *J. Agric. Food Chem.* **1987**, *35*, 884−889.

(6) Strongman, D. B.; Miller, J. D.; Calhoun, L.; Findlay, J. A.; Whitney, N. J. *Bot. Mar.* **1987**, *30*, 21−26.

(7) Kasitu, G. C.; Apsimon, J. W.; Blackwell, B. A.; Fielder, D. A.; Greenhalgh, R.; Miller, J. D. *Can. J. Chem.* **1992**, *70*, 1308−1316.

(8) Machida, Y.; Nozoe, S. *Tetrahedron* **1972**, *28*, 5113−5117.

(9) Savard, M. E.; Blackwell, B. A.; Greenbalgh, R. *J. Nat. Prod.* **1986**, *52*, 1267−1278.

(10) Desjardins, A. E.; Hohn, T. M.; McCormick, S. P. *Microbiol. Rev.* **1993**, *57*, 595−604.

(11) Kimura, M. T. T.; O'Donnell, K.; Ward, T. J.; Fujimura, M.; Hamamoto, H.; Shibata, T.; Yamaguchi, I. *FEBS Lett.* **2003**, *539*, 105−110.

(12) Pedersen, P. B.; Miller, J. D. *Nat. Toxins* **1999**, *7* (6), 305−9.

(13) Dowd, P. F.; Miller, J. D.; Greenhalgh, R. *Mycologia* **1989**, *81*, 646−650.

(14) Wang, Y. Z.; Miller, J. D. *J. Phytopathol.* **1988**, *122*, 118−125.

(15) Streit, E.; Schwab, C.; Sulyok, M.; Naehrer, K.; Krska, R.; Schatzmayr, G. *Toxins* **2013**, *5*, 504−523.

(16) Hanson, J. R.; Nyfeler, R. *J. Chem. Soc., Perkin Trans. 1* **1976**, 2471−2475.

(17) McCormick, S. P.; Alexander, N. J.; Harris, L. J. *Appl Environ Microbiol* **2010**, *76*, 136−41.

(18) Allen, M. S.; Darby, N.; Salisbury, P.; Money, T. *Tetrahedron Lett.* **1978**, *26*, 2255−2256.

(19) Gardiner, D. M.; Kazan, K.; Manners, J. M. *Mol. Plant-Microbe Interact.* **2009**, *22*, 1588−1600.

(20) Frandsen, R. J. N.; Frandsen, M.; Giese, H. In *Plant Fungal Pathogens: Methods and Protocols*; Bolton, D.; Thomma, B. P. H. J., Eds.; Springer Science, 2012; Vol. *835*, pp 17−45.

(21) Hutchins, P. M.; Moore, E. E.; Murphy, R. C. *J. Lipid Res.* **2011**, *52* (11), 2070−2083.

(22) Grossert, J. S.; Herrera, L. C.; Ramaley, L.; Melanson, J. E. *J. Am. Soc. Mass Spectrom.* **2014**, *25* (8), 1421−1440.

(23) Cohen, H.; Charrier, C.; Ricard, L.; Perreau, M. I. *J. Nat. Prod.* **1992**, *55*, 326−332.

(24) Barton, D. H. R.; Werstiuk, N. H. *J. Chem. Soc. C* **1968**, 148−155.

(25) Alam, M.; Gareth Jones, E. B.; Bilayet Hossain, M.; Van der Helm, D. *J. Nat. Prod.* **1996**, *59*, 454−456.

(26) Desjardins, A. E.; Proctor, R. H.; Bai, G.; McCormick, S. P.; Shaner, G.; Buechley, G.; Hohn, T. M. *Mol. Plant-Microbe Interact.* **1996**, *9*, 775−781.

(27) Harris, L. J.; Desjardins, A. E.; Plattner, R. D.; Nicholson, P.; Butler, G.; Young, J. C.; Weston, G.; Proctor, R. H.; Hohn, T. M. *Plant Dis.* **1999**, *83*, 954−960.

(28) Jansen, C.; von Wettstein, D.; Kogel, K. H.; Felk, A.; Maier, F. J. *Proc. Natl. Acad. Sci. U. S. A.* **2005**, *102*, 16892−16897.

(29) Frandsen, R. J. N.; Anderson, J. A.; Kristensen, M. B.; Giese, H. *BMC Mol. Biol.* **2008**, *9*, 70.

(30) Xue, A. G.; Armstrong, K. C.; Voldeng, H. D.; Fedak, G.; Babcock, C. *Can. J. Plant Pathol.* **2004**, *26*, 81−88.

(31) Leslie, J.; Summerell, B., In *Fusarium Laboratory Manual*; Blackwell Publishing, 2006.

(32) Miller, J. D.; Blackwell, B. A. *Can. J. Bot.* **1986**, *64*, 1−5.